J|A|C|S COMMUNICATIONS

Published on Web 04/07/2009

Sensitivity Enhancement in Static Solid-State NMR Experiments via Single- and Multiple-Quantum Dipolar Coherences

T. Gopinath and Gianluigi Veglia*

Department of Chemistry and Department of Biochemistry, Molecular Biology, and Biophysics, University of Minnesota, Minneapolis, Minnesota 55455

Received January 6, 2009; E-mail: vegli001@umn.edu

NMR spectroscopy is inherently a low-sensitivity technique.[1] In spite of the technology advancements in high-field magnets, hardware, and isotopic enrichments, many hours or several days of signal averaging are required to collect the data in multidimensional experiments for biomacromolecules. For liquid-state NMR, sensitivity enhancement (SE) pulse schemes represented a breakthrough.[2,3] In combination with transverse-relaxation-optimized spectroscopy (TROSY),[4] SE methods have dramatically improved both the sensitivity and resolution of NMR spectra, enabling the analysis of macromolecular systems with masses greater than 80 kDa.[5−7] While these developments involved mostly liquid-state NMR techniques, static and magic-angle-spinning (MAS) solid-state NMR experiments could in principle profit from them. For instance, TROSY-like effects have recently been observed in solid-state NMR spectra of proteins,[8−10] and some SE schemes have also been introduced for solids.[11,12] However, these methods have not been fully developed for solids.

Here we report the first example of SE via single- and multiple-quantum dipolar coherences for a net gain in signal-to-noise ratio (S/N) of up to 40%. We implemented the SE scheme for the polarization inversion spin exchange at magic angle (PISEMA) experiment, a separated local field (SLF) experiment that correlates the dipolar coupling (DC) and chemical shift anisotropy (CSA) in two dimensions for static solid-state NMR spectroscopy.[13,14] SLF experiments have been widely applied for determining the interactions of peptides and proteins with membranes, elucidating the structure and topology of membrane proteins in aligned lipid bilayers, and analyzing liquid-crystalline molecules.[15−26]

This new implementation is different from the liquid-state NMR SE technique and previous solid-state NMR schemes. In fact, the earlier SE schemes[2,3] detect two orthogonal components of *chemical-shift-modulated* coherences, enhancing the signal-to-noise ratio (S/N) by a factor of $\sqrt{2}$ or 40%. In contrast, our new approach detects two *dipolar-modulated* coherences encoded in single- and multiple-quantum coherences. The pulse scheme presented here (sensitivity-enhanced PISEMA or SE-PISEMA) increases the sensitivity of the original experiment up to 40% (Figure 1).

In the conventional PISEMA experiment (Figure 1A),[13] a cross-polarization period from the abundant spins I (^{1}H) to the S spins (^{15}N) is followed by a 35° pulse on the I spins, which flips the magnetization along the magic angle (54.3°). Spin exchange between the I and S spins is then established during t_1 evolution by applying a frequency-switched Lee−Goldburg (FSLG) homonuclear decoupling sequence[27] on the I spins synchronously with 180° phase-shifted 2π pulses on the S spins, satisfying the Hartmann−Hann condition.[28] As a result, the spin diffusion among I spins and the S-spin chemical shift evolution are suppressed, giving rise to a scaled heteronuclear DC evolution. For an I−S spin system, the density matrix (ρ) during t_1 evolution of the PISEMA experiment can be described in the doubly tilted rotating

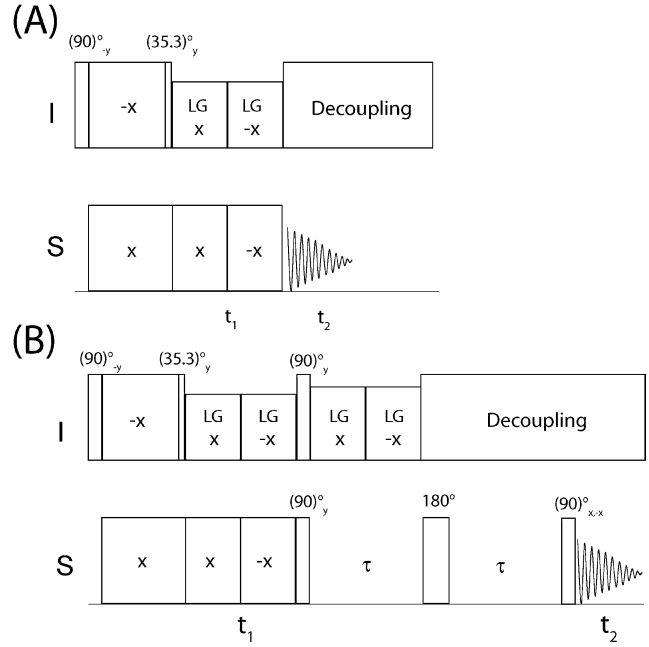

Figure 1. Pulse sequences for the (A) conventional PISEMA and (B) SE-PISEMA experiments.

frame defined by the operator $U = \exp(-i\theta_m I_y) \exp(-iS_y\pi/2)$ in the following form:[29,30]

$$\rho(t_1) = (I_z - S_z)\cos[(\sin\theta_m)\omega_{IS}t_1] - (2I_yS_x - 2I_xS_y)\sin[(\sin\theta_m)\omega_{IS}t_1] \quad (1)$$

where $\omega_{IS} = 2\pi D_{IS}$ and D_{IS} is the heteronuclear DC. When the S spin operators are converted to the laboratory frame by applying a 90°$_y$ rotation, the above equation can be rewritten as

$$\rho(t_1) = (I_z - S_x)\cos[(\sin\theta_m)\omega_{IS}t_1] + (2I_yS_z + 2I_xS_y)\sin[(\sin\theta_m)\omega_{IS}t_1] \quad (2)$$

After t_1 evolution, S_x is detected under I-spin decoupling, and the final density matrix for a PISEMA experiment with two scans for each t_1 increment is given by

$$\rho_{PISEMA} = -2S_x\cos[(\sin\theta_m)\omega_{IS}t_1]e^{i\omega_S t_2} \quad (3)$$

where ω_S represents the chemical shift of the S spin. From these equations, it is apparent that the conventional PISEMA experiment detects *only* the cosine-modulated dipolar coherence, while the sine-modulated coherence is encoded in the unobservable two-spin-order term.

10.1021/ja900096d CCC: $40.75 © 2009 American Chemical Society

In the SE-PISEMA experiment (Figure 1B), t_1 evolution (eq 2) is followed by a 90° pulse on the I and S spins, which converts the multiple-quantum term $2I_xS_y$ into the antiphase S-spin term $2I_zS_y$ and the S_x term into S_z. The resulting density matrix is given by

$$\rho[t_1 - (90)_y^{I,S}] = (I_x + S_z)\cos[(\sin\theta_m)\omega_{IS}t_1] + (2I_yS_x - 2I_zS_y)\sin[(\sin\theta_m)\omega_{IS}t_1] \quad (4)$$

During the time τ, the FSLG spin lock is continued on the I spins, giving rise to a scaled heteronuclear DC Hamiltonian $H_{IS} = (\cos\theta_m)\omega_{IS}2I_zS_z$. In this period, the S_z term does not evolve, whereas the antiphase S-spin operator evolves under H_{IS} as

$$2I_zS_y \rightarrow 2I_zS_y\cos[(\cos\theta_m)\omega_{IS}\tau] - S_x\sin[(\cos\theta_m)\omega_{IS}\tau]) \quad (5)$$

The other operators, I_x and $2I_yS_x$, evolve into unobservable two-spin-order terms and are neglected. The chemical shift evolution of the S spin during the first τ period is refocused by applying a π pulse followed by a second τ period under heteronuclear decoupling. Combining eqs 4 and 5 and considering only the single spin operators of S spin gives the following expression for the density matrix:

$$\rho[t_1 - (90)_y^{I,S} - \tau - \pi - \tau] = -S_z\cos[(\sin\theta_m)\omega_{IS}t_1] - \{\sin[(\cos\theta_m)\omega_{IS}\tau]\}S_x\sin[(\sin\theta_m)\omega_{IS}t_1] \quad (6)$$

In eq 6, sign inversion due to the π pulse is taken into account. At this point, a final $\pi/2$ pulse is applied on the S spin with phases x and $-x$ in two separate scans, followed by S-spin detection under I-spin decoupling. *This scheme allows one to detect both sine and cosine dipolar coherences*. The resulting FIDs (stored in separate files) can be described by the density matrices ρ_1 and ρ_2:

$$\begin{aligned}\rho_1 &= \rho[t_1 - (90)_y^{I,S} - 2\tau - (90)_x - t_2] \\ &= (S_y\cos[(\sin\theta_m)\omega_{IS}t_1] - \{\sin[(\cos\theta_m)\omega_{IS}\tau]\} \times S_x\sin[(\sin\theta_m)\omega_{IS}t_1])e^{i\omega_S t_2} \\ \rho_2 &= \rho[t_1 - (90)_y^{I,S} - 2\tau - (90)_{-x} - t_2] \\ &= (-S_y\cos[(\sin\theta_m)\omega_{IS}t_1] - \{\sin[(\cos\theta_m)\omega_{IS}\tau]\} \times S_x\sin[(\sin\theta_m)\omega_{IS}t_1])e^{i\omega_S t_2}\end{aligned} \quad (7)$$

Addition and subtraction of the two density matrices gives the following sine (ρ_s) and cosine (ρ_c) terms, respectively:

$$\begin{aligned}\rho_s &= \rho_1 + \rho_2 = -2\{\sin[(\cos\theta_m)\omega_{IS}\tau]\}S_x\sin[(\sin\theta_m)\omega_{IS}t_1]e^{i\omega_S t_2} \\ \rho_c &= \rho_1 - \rho_2 = 2S_y\cos[(\sin\theta_m)\omega_{IS}t_1]e^{i\omega_S t_2}\end{aligned} \quad (8)$$

Unlike the original PISEMA experiment, the SE-PISEMA scheme detects and also uncouples the sine- and cosine-modulated coherences by performing a two-step phase cycle of the last 90° pulse followed by addition and subtraction of the resultant data sets. It should be noted that in the SE-PISEMA pulse sequence, ρ_c and ρ_s are phase-shifted by 90° in both dimensions. Therefore, a relative 90° zero-order phase correction after Fourier transformation must be applied to obtain the pure absorptive phase in both dimensions of ρ_c and ρ_s.[2] In the sine-modulated term, the dipolar doublet peaks associated with each S spin have opposite signs. As a result, the addition or subtraction of the absorptive-phase two-dimensional data sets ρ_c and ρ_s yields a two-dimensional spectrum in which the intensity of one component of the dipolar doublet is increased by a factor of $\{1 + \sin[(\cos\theta_m)\omega_{IS}\tau]\}$ and that of the other component decreased by a factor $\{1 - \sin[(\cos\theta_m)\omega_{IS}\tau]\}$ compared with the corresponding resonances in the PISEMA experiment (eq 3). The resulting density matrix for the SE-PISEMA scheme is obtained by subtracting ρ_s from ρ_c:

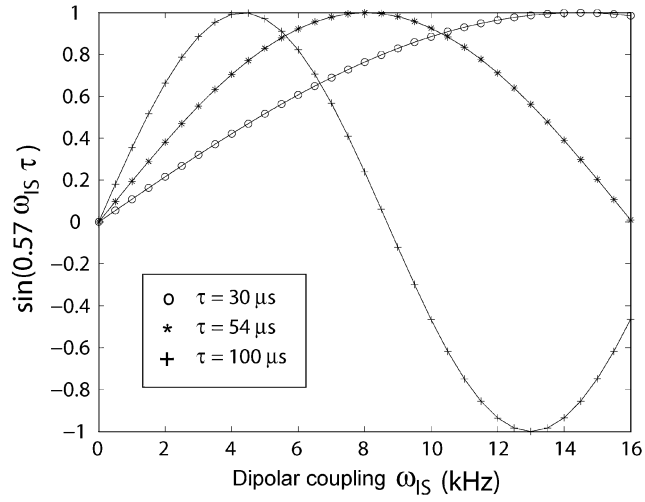

Figure 2. (A) Simulations of the $\sin[(\cos\theta_m)\omega_{IS}\tau]$ factor as a function of the DC values for the SE-PISEMA experiment. For $\tau = 54\ \mu s$, the maximum sensitivity enhancement is achieved with $D_{IS} \approx 8$ kHz.

$$\rho_{SE\text{-}PISEMA} = \rho_c(\omega_1, \omega_2) - \rho_s(\omega_1, \omega_2) \quad (9)$$

The rms noise of ρ_s and ρ_c is identical to that of ρ_{PISEMA}. As for the SE scheme in liquid-state NMR,[2] the addition or subtraction of two data sets [ρ_s and ρ_c, whose root-mean-square (rms) noises are uncorrelated] causes the noise level to increase by a factor of $\sqrt{2}$. Therefore, the S/N for the SE-PISEMA (eqs 8 and 9) and PISEMA (eq 3) experiments are related by the following equation:

$$(S/N)_{SE\text{-}PISEMA} = \frac{1 + \sin[(\cos\theta_m)\omega_{IS}\tau]}{\sqrt{2}}(S/N)_{PISEMA} \quad (10)$$

Since the S/N is a function of $\sin[(\cos\theta_m)\omega_{IS}\tau]$, the SE of the SE-PISEMA experiment depends on the value of τ and the DC values. For $\tau = 1/[(\cos\theta_m)4D_{IS}]$, the term $\sin[(\cos\theta_m)\omega_{IS}\tau]$ becomes equal to 1, and the SE has a maximum value of $\sqrt{2}$ or 40%.

Figure 2 shows the theoretical values of $\sin[(\cos\theta_m)\omega_{IS}\tau]$ as a function of the DC. For $\tau = 54\ \mu s$, the $\sin[(\cos\theta_m)\omega_{IS}\tau]$ term is greater than 0.7 (with a maximum of 1.0) for DCs ranging from 4 to 12 kHz, giving rise to an SE range of 20−40%. It is noteworthy that the largest enhancements occur for values of D_{IS} greater than 5 kHz, which usually correspond to the DC values measured for the transmembrane domain resonances in oriented membrane protein samples.[15,19]

To demonstrate this new method, we performed PISEMA and SE-PISEMA experiments on a single crystal of ^{15}N-labeled *N*-acetylleucine (NAL). The two-dimensional spectra were acquired at 16.45 T using a Varian VNMRS spectrometer equipped with a flat-coil low-E probe, which was developed at the National High Magnetic Field Laboratory in Florida.[31]

Figure 3 shows the two-dimensional PISEMA and SE-PISEMA spectra of NAL. The fourfold symmetry of the crystal unit generates a set of four distinct resonances with different values of the CSA and DC. Table 1 summarizes the sensitivity enhancements for various peaks in the SE-PISEMA spectrum together with the corresponding theoretical values. The theoretical and experimental

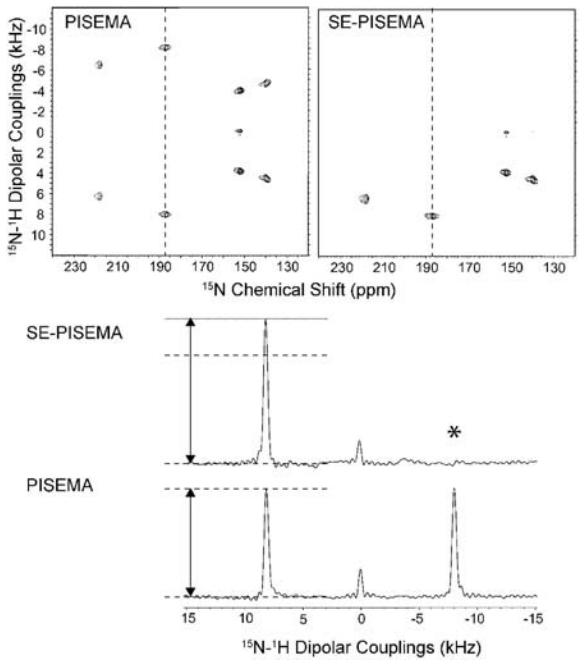

Figure 3. (top) Comparison of two-dimensional spectra of NAL from the (left) conventional PISEMA and (right) SE-PISEMA experiments. Both spectra were acquired with a cross-polarization time of 2 ms. The effective RF field during the t_1 period was 50 kHz on both channels. For SE-PISEMA, the effective field of FSLG during the τ period (54 μs) was 74 kHz. A total of eight scans and 64 increments of t_1 were used in each experiment. The dwell time in the indirect dimension was 40 μs, which corresponds to a spectral width of 30.4 kHz after adjustment of the theoretical scaling factor to 0.82.[14] The SE-PISEMA data set was divided by a factor of $\sqrt{2}$ to match the rms noise of the PISEMA experiment. (bottom) Comparison of one-dimensional slices from the two-dimensional experiments taken at 187 ppm. The asterisk indicates the cancellation of one of the dipolar doublet components due to the subtraction of the cosine- and sine-modulated spectra (see the text).

Table 1. Sensitivity Enhancements (S/N ratios) for the SE-PISEMA Experiment with Respect to the PISEMA Experiment for NAL Resonances

	sensitivity enhancement	
^{15}N chemical shift (ppm)	exptl	theor
139.7	1.27	1.27
152.1	1.20	1.18
187.0	1.33	1.40
218.0	1.38	1.37

values are in good agreement, with the resonances showing the highest DC values displaying the largest percent enhancements. For the two peaks resonating at 187 and 218 ppm, the SE is nearly at the maximum theoretical value of 40%. The slight deviations from the theoretical values are due to evolutions during finite $^{\pi}/_{2}$ and π pulses.

In conclusion, we have introduced a new approach for enhancing the sensitivity of static solid-state NMR experiments. In the PISEMA experiment, this method increases the S/N by up to 40%. In the last two decades, several SLF experiments have been developed and applied to various solid samples.[13] However, the low sensitivity of these experiments has drastically hampered the flourishing of these techniques. In combination with the enormous progress in probe technology[31] and sample preparations,[16] the implementation of our new SE method in several SLF experiments will speed up multidimensional data acquisition. This will expedite the determination of the structure and topology of membrane proteins, the analysis of membrane−ligand and membrane−protein interactions, and the high-resolution characterization of liquid crystals.

Acknowledgment. The authors acknowledge Dr. N. Traaseth for careful reading of the manuscript. This work was supported by grants to G.V. from the National Institutes of Health (GM64742, HL80081, GM072701).

References

(1) Ernst, R. R.; Bodenhausen, G.; Wokaun, A. In *Principles of Nuclear Magnetic Resonance in One and Two Dimensions*; Oxford Science Publications: Oxford, U.K., 1987.
(2) Cavanagh, J.; Rance, M. *J. Magn. Reson.* **1990**, *88*, 72–85.
(3) Kay, L. E.; Keifer, E.; Saarinen, T. *J. Am. Chem. Soc.* **1992**, *114*, 10663–10665.
(4) Pervushin, K.; Riek, R.; Wider, G.; Wuthrich, K. *Proc. Natl. Acad. Sci. U.S.A.* **1997**, *94*, 12366–12371.
(5) Tugarinov, V.; Hwang, P. M.; Kay, L. E. *Annu. Rev. Biochem.* **2004**, *73*, 107–146.
(6) Kreishman-Deitrick, M.; Egile, C.; Hoyt, D. W.; Ford, J. J.; Li, R.; Rosen, M. K. *Biochemistry* **2003**, *42*, 8579–8586.
(7) Fiaux, J.; Bertelsen, E. B.; Horwich, A. L.; Wuthrich, K. *Nature* **2002**, *418*, 207–211.
(8) Skrynnikov, N. R. *Magn. Reson. Chem.* **2007**, *45*, S161−S173.
(9) Chevelkov, V.; Faelber, K.; Schrey, A.; Rehbein, K.; Diehl, A.; Reif, B. *J. Am. Chem. Soc.* **2007**, *129*, 10195–10200.
(10) Vosegaard, T.; Bertelsen, K.; Pedersen, J. M.; Thogersen, L.; Schiott, B.; Tajkhorshid, E.; Skrydstrup, T.; Nielsen, N. C. *J. Am. Chem. Soc.* **2008**, *130*, 5028–5029.
(11) Tycko, R. *ChemPhysChem* **2004**, *5*, 863–868.
(12) Oliver, S. L.; Titman, J. J. *J. Magn. Reson.* **1999**, *140*, 235–241.
(13) Ramamoorthy, A.; Wei, Y.; Dong-Kuk, L. *Annu. Rev. NMR Spectrosc.* **2004**, *52*, 1–52.
(14) Wu, C. H.; Ramamoorthy, A.; Opella, S. J. *J. Magn. Reson.* **1994**, *109*, 270–272.
(15) Opella, S. J.; Marassi, F. M. *Chem. Rev.* **2004**, *104*, 3587–3606.
(16) Page, R. C.; Li, C.; Hu, J.; Gao, F. P.; Cross, T. A. *Magn. Reson. Chem.* **2007**, *45*, S2−S11.
(17) Traaseth, N. J.; Ha, K. N.; Verardi, R.; Shi, L.; Buffy, J. J.; Masterson, L. R.; Veglia, G. *Biochemistry* **2008**, *47*, 3–13.
(18) Dvinskikh, S. V.; Yamamoto, K.; Scanu, D.; Deschenaux, R.; Ramamoorthy, A. *J. Phys. Chem. B* **2008**, *112*, 12347–12353.
(19) Traaseth, N. J.; Verardi, R.; Torgersen, K. D.; Karim, C. B.; Thomas, D. D.; Veglia, G. *Proc. Natl. Acad. Sci. U.S.A.* **2007**, *104*, 14676–14681.
(20) Buffy, J. J.; Traaseth, N. J.; Mascioni, A.; Gor'kov, P. L.; Chekmenev, E. Y.; Brey, W. W.; Veglia, G. *Biochemistry* **2006**, *45*, 10939–10946.
(21) Traaseth, N. J.; Buffy, J. J.; Zamoon, J.; Veglia, G. *Biochemistry* **2006**, *45*, 13827–13834.
(22) Dvinskikh, S. V.; Durr, U. H.; Yamamoto, K.; Ramamoorthy, A. *J. Am. Chem. Soc.* **2007**, *129*, 794–802.
(23) Ramamoorthy, A.; Lee, D. K.; Santos, J. S.; Henzler-Wildman, K. A. *J. Am. Chem. Soc.* **2008**, *130*, 11023–11029.
(24) Waugh, J. S. *Proc. Natl. Acad. Sci. U.S.A.* **1976**, *73*, 1394–1397.
(25) Sinha, N.; Ramanathan, K. V. *Chem. Phys. Lett.* **2000**, *332*, 125–130.
(26) Muller, L.; Kumar, A.; Baumann, T.; Ernst, R. R. *Phys. Rev. Lett.* **1974**, *32*, 1402–1406.
(27) Bielecki, A.; Kolbert, A. C.; de Groot, H. j. M.; Griffin, R. G.; Levitt, M. H. *Adv. Magn. Reson.* **1990**, *14*, 111–124.
(28) Hartmann, S. R.; Hahn, E. L. *Phys. Rev.* **1962**, *128*, 2042–2053.
(29) Gan, Z. *J. Magn. Reson.* **2000**, *143*, 136–143.
(30) Fu, R.; Tian, C.; Kim, H.; Smith, S. A.; Cross, T. A. *J. Magn. Reson.* **2002**, *159*, 167–174.
(31) Gor'kov, P. L.; Chekmenev, E. Y.; Li, C.; Cotten, M.; Buffy, J. J.; Traaseth, N. J.; Veglia, G.; Brey, W. W. *J. Magn. Reson.* **2007**, *185*, 77–93.

JA900096D